Conformational Modulation of Electron Transfer within Electrostatic Porphyrin: Cytochrome *c* Complexes

Randy W. Larsen,*,† Dawn H. Omdal,† Ravi Jasuja,† Shui Lin Niu,† and David M. Jameson‡

Departments of Chemistry and Biochemistry and Biophysics, University of Hawaii at Manoa, 2545 The Mall, Honolulu, Hawaii 96822

The present study examines photoinduced electron transfer within self-assembled complexes between cytochrome *c* and either free base uroporphyrin (URO) or free base tetrakis(4-carboxyphenyl)porphyrin (4CP). In both systems, complexation of the porphyrin to the protein results in bathochromic shifts in the absorption bands of the porphyrin. Interestingly, equilibrium circular dichroism data demonstrate significant differences in the orientation of the bound porphyrins. The effect of orientational differences on photoinduced electron transfer between the bound porphyrin and the heme group of cytochrome *c* are demonstrated in the steady-state and time-resolved fluorescence and triplet−triplet transient absorption data obtained for the two complexes. In the case of the cytochrome *c*−4CP complex, the singlet state of the 4CP is significantly quenched by the heme group of the protein. Analysis of the time-resolved fluorescence data reveals two discrete lifetime components at 9.3 (free 4CP) and 1.27 ns (bound 4CP). In contrast, the singlet state of URO is only moderately quenched by complexation to the protein. Fluorescence lifetime analysis reveals two components consisting of a discrete component at 15.7 ns (free URO) and a Lorentzian distribution of lifetimes centered at 3.8 ns. However, URO exhibits significant triplet-state quenching, resulting in intercomplex electron transfer in which the observed forward and reverse rates are similar ((1.8 ± 0.2) $\times 10^6$ and (1.6 ± 0.4) $\times 10^6$ s^{-1}, respectively). The difference in ET mechanism (i.e., singlet versus triplet) can be rationalized in terms of distinct dipole orientations of the bound porphyrins relative to the heme group of the protein. We further speculate that the orientational differences between bound URO and bound 4CP arise due to the flexibility of the URO side chains.

Introduction

Electron transfer (ET) reactions play a pivotal role in the catalytic cycles of a wide range of biologically important processes including nitrogen fixation, photosynthesis, and respiration.[1−5] Biological ET reactions occur between electrostatically stabilized protein−protein complexes and between various redox-active cofactors embedded within a single protein complex. Intramolecular ET rates are modulated by donor−acceptor distance, thermodynamic driving force, donor−acceptor orientation, the nature of the intervening medium, and both inner-sphere and outer-sphere reorganization.[6−14] The rates of intermolecular ET reactions require additional mechanistic steps described as (1) formation of the protein−protein complex, (2) ET between the redox centers of each protein within the complex, and (3) dissociation of the protein−protein complex. Thus, the rate of ET in such complexes may have an additional component to the overall reorganizational energy required for intermolecular ET that influences protein−protein recognition and docking (i.e., gating effects).[15−21]

Conformational dynamics associated with the interface between the donor and acceptor proteins have recently been suggested for complexes involving cytochrome *c* (Cc) and either cytochrome *c* peroxidase (CCP) or plastocyanin (PC).[15−21] In the case of intermolecular ET between ³ZnCc or ³SnCc and PC, the kinetic data could be explained using a model in which rearrangement of the proteins within the complex occurs after docking but prior to ET.[21] The corresponding back ET reaction

was not found to be gated. In the Cc/CCP system, it has been suggested that two docking sites are available on CCP for Cc which differ in their reactivity.[19] A model in which interconvertable conformational substrates within the complex regulate ET between the two proteins has been proposed to account for the presence of multiphasic kinetic data.

An alternative approach to the study of intermolecular ET in proteins involves the use of small photoactive molecules electrostatically bound to the docking region of redox proteins. Previous studies by Clark-Ferris and Fisher[22] and Zhou et al.[23] have demonstrated that anionic porphyrins can form complexes with Cc by forming electrostatic contacts with exterior lysines associated with the protein. The lysine residues believed to participate in complex formation are Lys 13, 27, 72, and 86. In addition, Zhou et al.[23] and Zhou and Rodgers[24] have shown that excitation of the bound photoactive uroporphyrins results in fixed-distance ET with rates that depend on solution ionic strength. Interestingly, the variation in ET rate with reaction driving force is consistent with semiclassical Marcus theory for the thermally activated back ET reaction while the photoinitiated forward reaction showed no inverted region with the same range of driving force. The lack of an inverted region was attributed to contributions from the coordinate solvent mode or to conformational gating.

In the present study, photoinduced ET within electrostatic complexes involving two structurally distinct anionic porphyrins and Cc have been examined. Equilibrium optical absorption and circular dichroism (CD) results presented here demonstrate that free base uroporphyrin (URO) and free base tetrakis(4-carboxyphenyl)porphyrin (4CP) form electrostatic complexes with Cc but with distinctive orientations (see Figure 1 for a structural diagram of these porphyrins). The effects of the

---

* To whom correspondence should be sent.
† Department of Chemistry.
‡ Department of Biochemistry and Biophysics.
⊗ Abstract published in *Advance ACS Abstracts,* September 1, 1997.

Conformational Modulation of Electron Transfer

J. Phys. Chem. B, Vol. 101, No. 40, 1997 **8013**

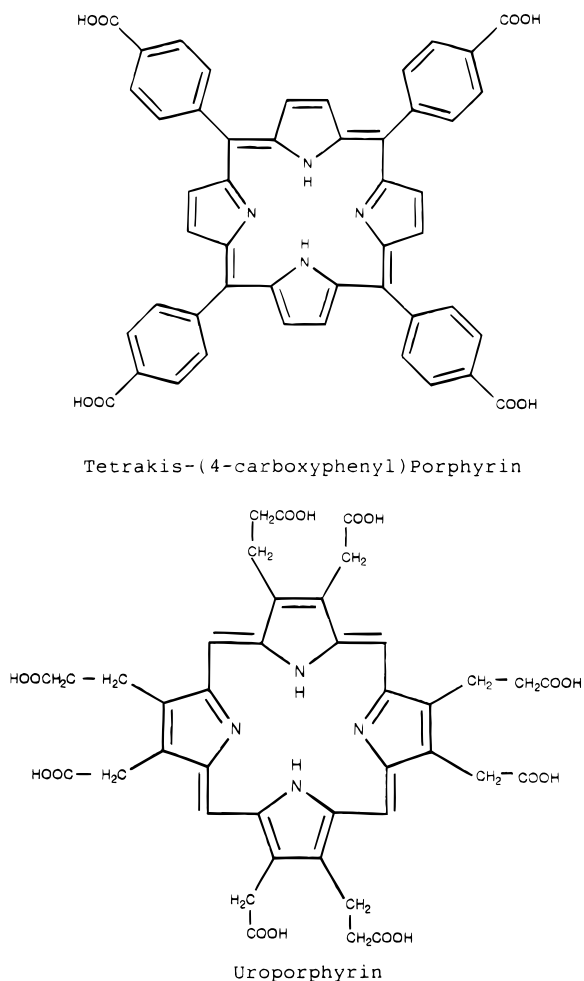Tetrakis-(4-carboxyphenyl)Porphyrin

Uroporphyrin

Figure 1. Structural diagrams of the porphyrins used in this study.

orientational differences on photoinduced ET between the bound porphyrin and the heme group of Cc are demonstrated in the steady-state and time-resolved fluorescence and triplet−triplet transient absorption data obtained for the two complexes. In the case of the Cc−4CP complex, the singlet state of the 4CP is significantly quenched by the heme group of the protein while the singlet state of URO is only moderately quenched by complexation to the protein. However, significant triplet-state quenching is observed for URO resulting in intercomplex ET. In addition, fluorescence lifetime analysis reveals two lifetime components for Cc−URO solutions consisting of a discrete component at 15.7 ns (free URO) and a Lorentzian distribution of lifetimes centered at 3.8 ns. These results demonstrate orientational control of intermolecular ET within the Cc−porphyrin complex and may arise due to the flexibility of the URO propionic and acetic acid side chains.

Materials and Methods

Bovine heart cytochrome *c* (Sigma), free base 4CP (Porphyrin Products, Logan UT), and free base URO (Porphyrin Products) were used without further purification. Cytochrome *c* stock solutions were prepared in 5 mM potassium phosphate buffer, pH 7.0. Porphyrin stock solutions (∼3 mM) were prepared in 0.1 M NaOH. The concentrations of the stock solutions were determined using $\epsilon_{550\ nm} = 19$ mM^{-1} cm^{-1} (cytochrome *c* reduced minus oxidized), $\epsilon_{552\ nm} = 18.3$ mM^{-1} cm^{-1} (URO diluted in 0.1 N HCl), and $\epsilon_{518\ nm} = 18.3$ mM^{-1} cm^{-1} (4CP diluted in 0.1 N HCl).[25,26]

Samples for difference measurements were prepared by diluting appropriate aliquots of the porphyrin and Cc to 10 μM

in 5 mM phosphate buffer, pH 7.0. One milliliter of each dilution was then placed in each side of a quartz tandem mixing cell (total path length was 1 cm) which was subsequently sealed with a Teflon cover and the absorption spectrum recorded. The tandem cell was then inverted to allow mixing of the porphyrin and protein. After a 20 min incubation period, the absorption spectrum of the combined protein−porphyrin solution was then recorded. The optical difference spectrum was obtained by subtracting the spectrum before mixing from the spectrum obtained after mixing.

Steady-state fluorescence quenching studies were performed by titrating aliquots of Cc from a stock solution into 1 mL of a 5 mM potassium phosphate buffer solution containing 25 μM porphyrin. Data were collected using an SLM 8000C spectrofluorometer (SLM Aminco, Champaign, IL) equipped with a red-sensitive R928 photomultiplier tube (Hamamatsu) and software from ISS (ISS, Inc., Champaign, IL). Excitation wavelengths were 610 and 628 nm for URO and 4CP, respectively, and emission was collected through a Schott RG645 filter. Data were corrected for dilution after each titration point.

Circular dichroism data were obtained by titrating aliquots of Cc from a stock solution into 1.5 mL of 12 μM porphyrin in a 0.5 cm quartz optical cell. The data were collected using a Jasco J600 spectropolarimeter interfaced to an IBM PC. Three traces were added and averaged for each spectrum.

Time-resolved fluorescence measurements were performed using an ISSK2 multifrequency and phase modulation spectrofluorometer equipped with an Ar ion laser (SpectraPhysics Model 2045) as the excitation source.[27] Data were collected using the 514 nm laser line, and emission at wavelengths greater than 570 nm was collected through a Schott RG082 filter. Sample concentrations were 15 μM for the porphyrins and 30 μM for Cc. Ethidium bromide was used as a calibration standard. Lifetime data were fit using software provided by ISS.

Triplet-state kinetics were examined using nanosecond transient absorption instrumentation described in detail elsewhere. Briefly, samples of porphyrin (20 μM) were excited at 532 nm using a pulsed Nd:YAG laser (Continuum SureLite II) with a pulse width of 7 ns (10 mW average power at 10 Hz). Changes in absorption were monitored using a Xe arc lamp (Oriel). The arc was overlapped with the pump laser in the sample cuvette and subsequently imaged onto the entrance slit of a Spex 1580 1/4M double monochromator. The light was detected using a thermoelectrically cooled R928 (Hamamatsu) photomultiplier tube. The signal was amplified using electronics of our own design and digitized using a Tektronix RTD710A 200 MHz transient digitizer. The data were then transferred to a 486-based microcomputer for further processing. Data fits were obtained using Enzfitter software.

Results

Steady-State Optical Absorption and Circular Dichroism Spectroscopy. Complexation of either URO or 4CP to Cc results in shifts in the absorption bands of the complexed porphyrin consistent with previous results. This is demonstrated by the absorption difference spectra shown in Figure 2.

The equilibrium CD spectrum of Cc in the Soret region displays a peak at 406 nm and a trough at 416 nm. The URO and 4CP, on the other hand, do not display CD in the Soret region due to the high symmetry of the conjugated macrocycle (D_{2h}). However, Figure 3 demonstrates that, upon complexation of the porphyrin to Cc, CD is induced in the bound chromophore. In addition, we do not find any evidence that
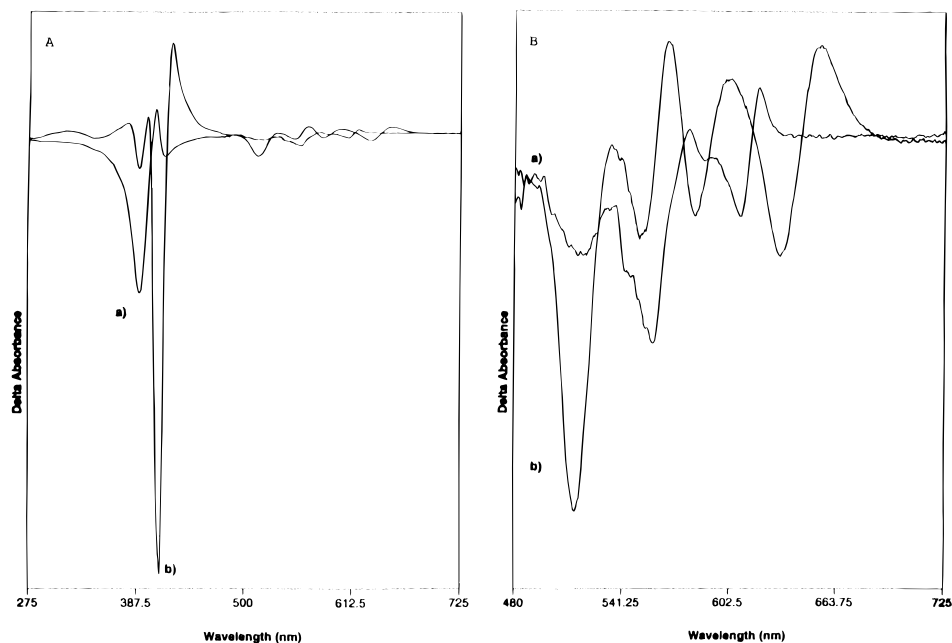
Figure 2. Optical difference spectra of porphyrin−Cc complexes in the Soret (A) and visible (B) regions. Trace a is the URO−Cc while trace b is the 4CP−Cc complex. Difference spectra are complexed minus uncomplexed using a 1 cm tandem mixing cell. Sample concentrations are 10 μM for both porphyrin and Cc.
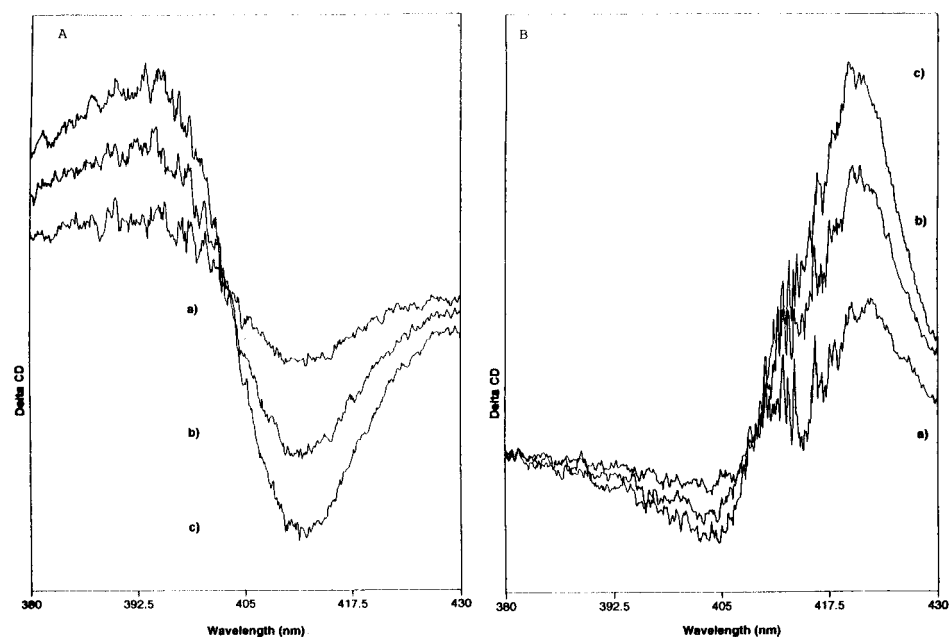

Figure 3. Circular dichroism difference spectra for the URO−Cc (A) and 4CP−Cc complexed (B). Difference spectra are complexed minus uncomplexed using a 1 cm quartz optical cuvette. Sample concentrations are 10 μM Cc and (a) 5, (b) 10, and (c) 15 μM porphyrin.

complexation perturbs the equilibrium electronic environment of the heme group or the protein tertiary structure (i.e., no observable conformational change in Cc upon porphyrin binding). From the CD difference spectra, it is apparent that URO displays positive/negative Cotton effects at 393 and 412 nm, respectively. In contrast, 4CP displays positive/negative Cotton effects at 420 and 403 nm, respectively. Binding constants obtained from the CD titrations are $(1.72 \pm 0.7) \times 10^4$ and $(1.55 \pm 0.3) \times 10^4$ M^{-1} for URO and 4CP, respectively.

Steady-State Fluorescence Quenching. In the absence of Cc, both URO and 4CP exhibit intense fluorescence emission when excited at either 610 (URO) or 628 nm (4CP). The emission maxima were found to be 620 and 643 nm for URO and 4CP, respectively. Addition of Cc to solutions containing either porphyrin results in significant quenching of the porphyrin

singlet state. The corresponding Stern−Volmer plot (Figure 4) displays upward curvature for both porphyrins, indicating ground-state complex formation. The data further demonstrate a greater degree of quenching of 4CP emission in the presence of Cc relative to the quenching of URO fluorescence. The Stern−Volmer plot for the quenching of the 4CP singlet state by Cc could be fit using the following equation:[28]

$$I_0/I = (1 + K_a[Q])(1 + K_{SV}[Q]) \qquad (I)$$

where K_a is the association constant of the complex, [Q] is the concentration of the added quencher, and K_{SV} is the Stern−Volmer constant and is equal to $k_q t_0$, where k_q is the quenching constant and t_0 is the singlet state lifetime in the absence of quencher. The best fit gave $K_a = (2.73 \pm 0.3) \times 10^4$ M^{-1} and

Conformational Modulation of Electron Transfer

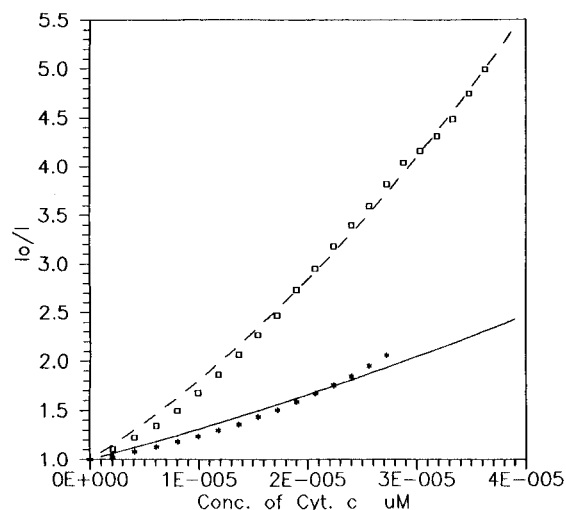*J. Phys. Chem. B, Vol. 101, No. 40, 1997* **8015**

Figure 4. Stern–Volmer plot of porphyrin singlet-state quenching by Cc: (□) quenching of the 4CP singlet and (∗) quenching of the URO singlet. The solid line represents the best fit to the Stern–Volmer equation that considers both static and dynamic quenching. Initial porphyrin concentration was 5 μM.

$K_{SV} = (4.17 \pm 0.25) \times 10^1$ M^{-1}. Interestingly, the data for the quenching of the singlet state of URO also displays upward curvature, but an adequate fit to eq I could not be obtained. The lack of an adequate fit to eq I may be due to the presence of multiple quenching components (see below).

Time-Resolved Fluorescence. Figure 5 displays the results of fluorescence lifetime analysis of 4CP and URO in the absence and presence of Cc. In the absence of the protein, 4CP and URO display discrete singlet-state lifetimes of 9.3 and 15.7 ns, respectively. In the presence of ferriCc, the fluorescence lifetime data for 4CP could be fit to two discrete components at 9.3 and 1.27 ns. These values correspond to 4CP that remains uncomplexed (9.3 ns component) and to 4CP that is complexed to the protein (1.27 ns component). Using the value of 9.3 ns for the natural lifetime of 4CP and the K_{SV} value obtained above, k_q is calculated to be 2.7×10^9 M^{-1} s^{-1}.

In contrast, fluorescence lifetime data obtained for URO in the presence of Cc could not be fit to two discrete lifetime components. However, the data fit well to a discrete component at 15.7 ns and to a Lorentzian distribution of lifetimes centered at 3.8 ns. These values correspond to uncomplexed (15.7 ns component) and complexed (3.8 ns distribution) URO. The fact that the quenched URO is present as a distribution implies that a range of k_q values exists for quenching and explains the lack of an adequate fit to eq I (Stern–Volmer analysis).

Porphyrin Triplet-State Quenching. Both 4CP and URO exhibit long-lived triplet states in the absence of Cc with decay rate constants of $(1.6 \pm 0.01) \times 10^3$ and $(1.1 \pm 0.01) \times 10^3$ s^{-1}, respectively. Addition of Cc to a solution containing either 4CP (Figure 6, Panel A) or URO (Figure 7, Panel A) results in significant quenching of the triplet state. In the case of URO, the triplet-state decay becomes increasingly biphasic as the concentration of Cc is increased during the titration. In contrast, the triplet decay of 4CP remains monophasic throughout the titration. A plot of the triplet decay rate of 4CP versus Cc concentration (Figure 8) indicates that the quenching reaction is second order with a rate constant of $(2.3 \pm 0.03) \times 10^9$ M^{-1} s^{-1} and is consistent with the value previously reported by Cho et al.[29] Examination of the URO data reveals that only the slow phase of the triplet-state decay is dependent upon Cc concentration with a second-order rate constant of $(1.83 \pm 0.03) \times 10^9$ M^{-1} s^{-1}. The fast-phase rate constant does not show any
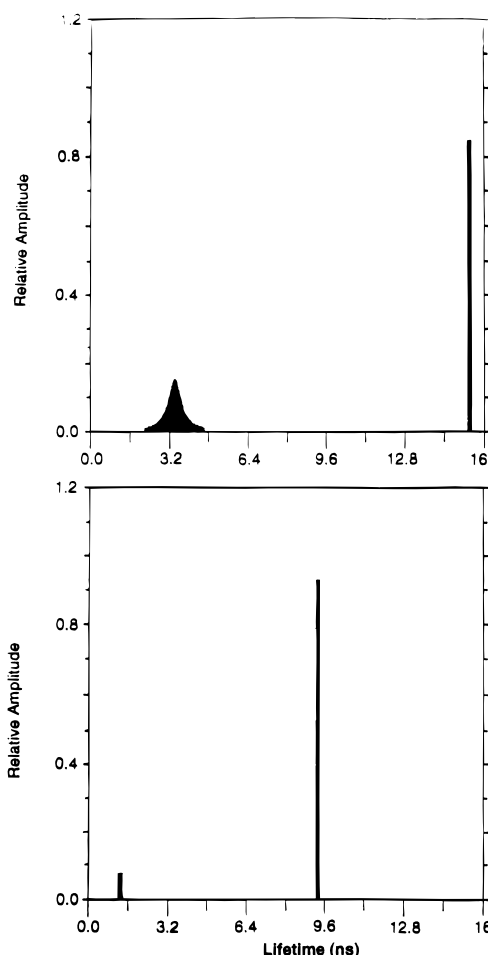

Figure 5. Lifetime analysis for the quenching of URO (top panel) and 4CP (bottom panel) in the presence of Cc. See text for details of the fit.

concentration dependence, indicating a first-order process with a rate constant of $(1.7 \pm 0.4) \times 10^6$ s^{-1}.

Absorption changes in the visible region of the spectrum were also examined to probe the rate of ET between the porphyrins and Cc. Reduction of the heme group of Cc results in a significant increase in absorbance at 550 nm ($\Delta\epsilon = 19$ mM^{-1} cm^{-1}) which can be monitored to determine the rate of ET. In addition, the change in absorbance at 556 nm (isosbestic point between reduced and oxidized Cc) was also examined to determine the extent to which triplet–triplet absorption from the porphyrin contributes to the change in absorbance at 550 nm. The results are summarized in Figures 6B (4CP/Cc system), 7B and 9 (URO/Cc system). For the 4CP/Cc system, no changes in absorbance at 550 nm due to reduction could be observed.

In contrast, significant changes in absorbance are observed at 550 nm in the presence of URO and varying concentrations of Cc. At low concentrations of Cc, the absorbance at 550 nm increases above the preflash level, which subsequently decays back to the preflash level on longer time scales. The concentration-dependent rate of absorbance increase at 550 nm parallels the concentration-dependent rate of the slow-phase triplet decay at 434 nm. At higher Cc concentrations, the absorbance change at 550 nm is also biphasic but the rate constants for the absorbance increase and subsequent decrease no longer show a dependence on Cc concentration. The rate constants are found to be $(1.8 \pm 0.4) \times 10^6$ and $(1.6 \pm 0.2) \times 10^6$ s^{-1} for the absorbance increase and subsequent decrease, respectively. It should be noted that the rate of the absorbance increase at 550
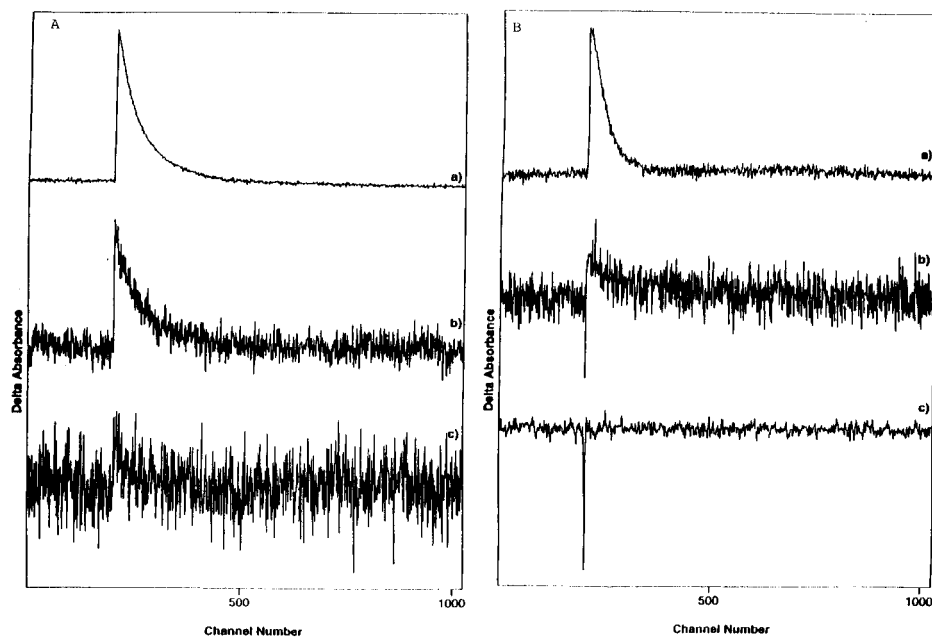
Figure 6. Triplet−triplet transient absorption of 4CP in the presence of varying concentrations of Cc obtained at 434 (A) and 550 nm (B): (a) 4CP only, (b) 30 mM Cc, and (c) 60 mM Cc. The time scales for the various traces are as follows: (a) 10, (b) 0.2, and (c) 0.2 ms/channel. The concentration of 4CP was maintained at 15 mM. Samples were obtained using a 1 cm quartz optical cuvette.
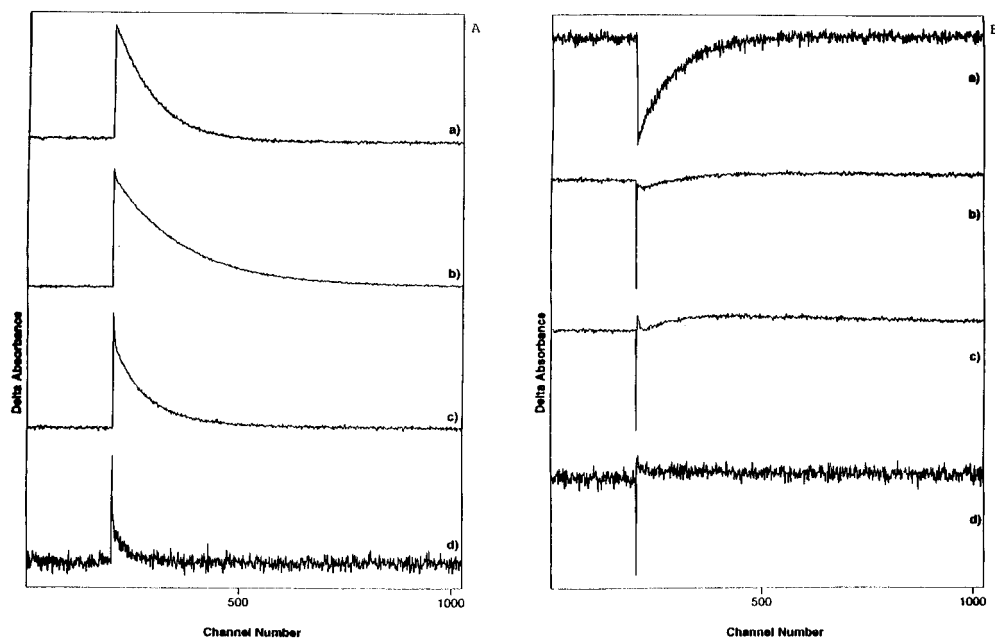

Figure 7. Triplet−triplet transient absorption of URO in the presence of varying concentrations of Cc obtained at 434 (A) and 550 nm (B): (a) URO only, (b) 30 mM Cc, and (c) 60 mM Cc. The time scales for the various traces are as follows: (a) 25, (b) 0.2, and (c) 0.2 ms/channel. The concentration of URO was maintained at 15 mM. Samples were obtained using a 1 cm quartz optical cuvette.

nm at high Cc concentration ($(1.8 \pm 0.4) \times 10^6$ s^{-1}) is nearly identical with the rate constant for the fast-phase triplet decay ($(1.7 \pm 0.4) \times 10^6$ s^{-1}) observed with the same Cc concentration. These results suggest that with low concentrations of Cc the triplet-state quenching of URO is dominated by bimolecular ET between the excited-state porphyrin and the heme group of Cc. As the concentration of Cc is increased, the concentration of the URO/Cc electrostatic complex also increases and intracomplex ET dominates.

Discussion

Steady-State Complex Formation between Anionic Porphyrins and Cc. Cytochrome *c* forms electrostatic complexes with a number of proteins including cytochrome *c* oxidase

(CcO), cytochrome *c* reductase (CcR), cytochrome *c* peroxidase (CcP), plastocyanin (Pc), and ferrodoxin.[15] Complex formation involves electrostatic interaction between a region of positively charged lysine residues located on the exterior of the Cc with a complimentary region of negatively charged carboxylic acid groups located on the exterior of the complex partner. Extensive investigation has led to the conclusion that the lysine residues that make the most significant contributions to complex formation are Lys 13, 27, 72, and 87.[30,31] The orientation of the exterior lysines establishs a dipole which is complimentary to that of the corresponding partner (CcO, CcR, CCP, etc.).[20]

Clark-Ferris and Fisher[22] and Zhou et al.[23] have shown that the anionic porphyrins 4CP and URO also bind to Cc in the same region as the physiological docking partners. The binding

Conformational Modulation of Electron Transfer

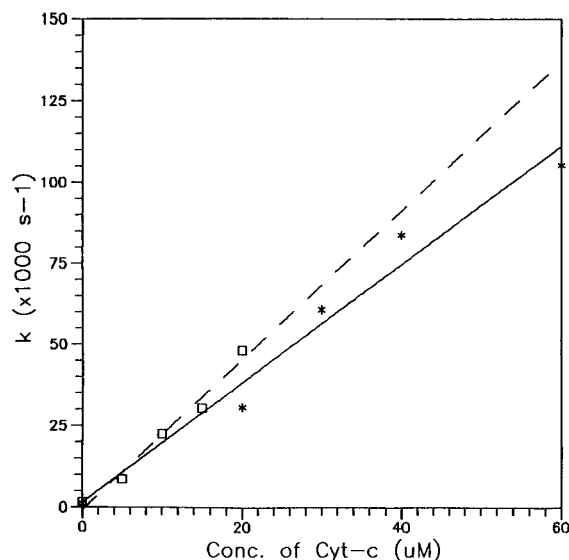*J. Phys. Chem. B, Vol. 101, No. 40, 1997* **8017**

Figure 8. Stern−Volmer plot for the triplet-state quenching of 4CP (□) and URO (*) by Cc. Best-fit lines are also displayed for each data set.

constant for both porphyrins is on the order of 1.5×10^4 M^{-1} under low ionic strength conditions. Complexation is accompanied by a red-shift in the optical absorption bands of the porphyrin while the spectral properties of Cc are unaffected. The CD data presented here further demonstrate that complexation of the porphyrin to Cc results in induced CD (ICD) associated with the bound porphyrin. Examination of the shape of the ICD spectra reveal that, although both porphyrins bind to the same region, their orientations are quite distinct.

To evaluate the orientational dependence of ICD, it is necessary to understand the origin of the ICD in the bound porphyrin. Due to the high symmetry of the free base porphyrins (D_{2h}), no intrinsic CD is expected or observed. However, complexation of the porphyrin with a chiral molecule (e.g., proteins/peptides) induces a CD in the bound porphyrin. The induction of CD into a symmetric molecule (e.g., free base porphyrin) arises from (1) coupling of an electronic transition moment of one chromophore with the magnetic dipole transition on the other chromophore ($\mu-\mu$ mechanism), (2) perturbation of the electronic and magnetic moments of a chromophore by an external static field (also known as the Erying one-electron theory), or (3) coupling of the electronic transition moments of two different chromophores ($\mu-\mu$ mechanism also known as the coupled oscillator model).[32] In describing ICD associated with symmetrical heme groups in hemoglobin and myoglobin, Hso and Woody suggested that the most likely mechanism of ICD is the coupled oscillator model.[33] This argument is based upon the fact that a given Coulombic potential is ineffective in inducing optical rotation in highly symmetrical chromophores. In addition, it was suggested that the heme group is surrounded on all sides by a large number of charged residues, which would lead to the canceling out of ICD effects originating from a static field induced by these charges. Within the coupled oscillator theory, the ICD in the heme group was attributed to the coupling of the porphyrin $\pi-\pi^*$ transition with a $\pi-\pi^*$ transition of a nearby aromatic amino acid. More recent studies have also suggested that $\pi-\pi^*$ transitions associated with protein backbone carbonyls can also couple to porphyrin $\pi-\pi^*$ transitions also giving rise to ICD.[33]

In the present case, the bound porphyrins are in close proximity to one aromatic amino acid (Phe 82), which is partially exposed in the proposed binding region, and to peptide carbonyls, all of which may contribute to ICD. In addition,

coupling of the electronic transitions associated with the intrinsic heme group of Cc with that of the bound porphyrin may make a significant contribution to ICD. This is because the heme edge is exposed at the region of porphyrin binding. Thus, close spatial interactions that facilitate electronic coupling are likely to be present between the bound porphyrin and the heme group. It must also be considered that not only is the distance between two centers important in ICD but also the magnitude of the transitions moments of the two interacting chromophores. From these observations, the ICD associated with the bound porphyrin is most likely due to heme-porphyrin dipole coupling since these transition moments are significantly larger than those of either the aromatic amino acid or backbone carbonyl groups.

If the electronic coupling between the bound porphyrin and the intrinsic heme group of Cc is the dominant term in ICD (as expected), then the difference in the shape of the ICD between bound URO and bound 4CP represents differences in orientation of the bound chromophores relative to the transition moment of the heme. This suggests that although both porphyrins bind a similar region on Cc they bind with significantly different orientations. The presence of both a negative and a positive Cotton effect in porphyrins has been explained by differences in coupling between the x- and y-transition moments associated with the porphyrin Soret transition relative to the coupling chromophore.[33,34] The fact that bound URO and bound 4CP have both positive and negative Cotton effects but different signs suggests a similar coupling mechanism with the transition moments for the x- and y-polarized transitions in 4CP being oriented 90° relative x- and y-polarized transitions in URO.

Porphyrin Excited-State Quenching. The effects of surface orientation on the excited-state properties of the bound porphyrins is pronounced. Photoexcitation of the bound porphyrins (either 4CP or URO) results in formation of both singlet and triplet excited states that are quenched in the presence of Cc. Time-resolved fluorescence measurements suggest that the bound forms of each porphyrin contain a population of molecules in which the singlet state is quenched by the heme group of Cc. However, the quenching rates as well as the relative populations of molecules with quenched singlet states are distinct between the two porphyrins. Comparison of the two quenched lifetimes (obtained from time-resolved fluorescence data) reveals a quenching rate for 4CP ($k = 1/\tau_q - 1/\tau_0$) that is twice as large than that of the URO (1.07×10^8 and 6.37×10^7 s^{-1} for 4CP and URO, respectively). The corresponding Stern−Volmer analysis suggests that the bound 4CP is more efficiently quenched than the bound URO. In addition, the yield of triplet state associated with 4CP is significantly reduced in the presence of Cc, which is a result of the rapid decay of the singlet state. In contrast, URO exhibits higher yields of triplet state with the triplet state being quenched by the heme group of Cc with a rate constant of ~1.8×10^6 s^{-1}. Thus, the orientation of the bound 4CP favors singlet-state quenching while the orientation of the bound URO favors triplet-state quenching.

Quenching of the porphyrin singlet excited state by Cc may occur through energy transfer to the heme, electron transfer to the heme, or both. The rate of energy transfer can be estimated using the following equation:[35]

$$k_T = (1/\tau_o)(R_o/R)^{-6}$$

where τ_o is the lifetime of the fluorophore in the absence of quencher, R is the distance between the donor and acceptor (~13 Å in this case), and R_o is the distance at which the energy transfer occurs with an efficiency of 50% and can be expressed as
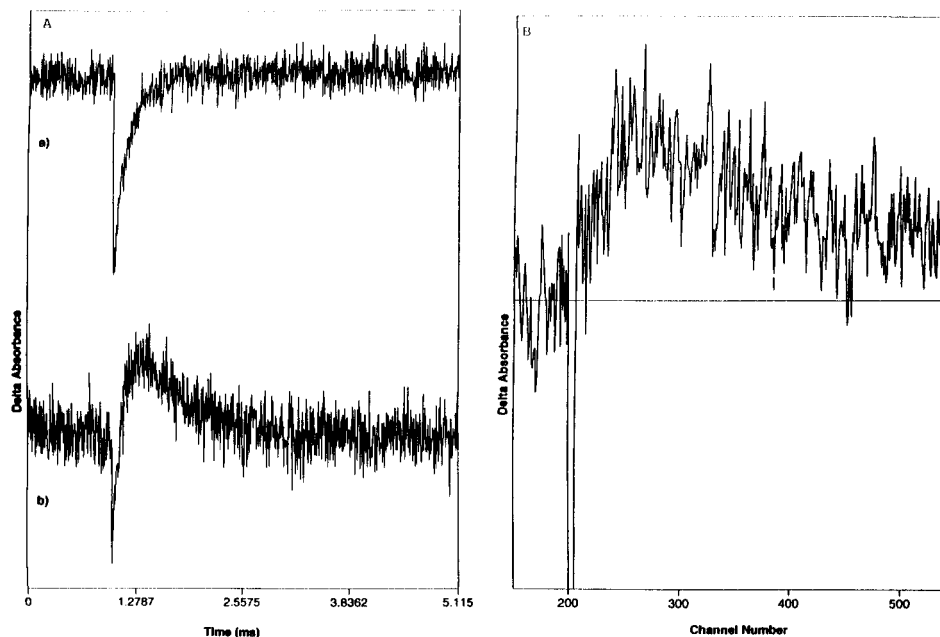
Figure 9. Transient absorption of URO (15 mM) in the presence of Cc (35 mM) obtained at 550 (A, trace b, and B) and 556 nm (A, trace a). The time scale for (B) is 10 ns/channel. The concentration of URO was maintained at 15 mM. Samples conditions are the same as in Figures 5 and 6.

$$R_{\mathrm{o}} = 9.7 \times 10^3 (J\kappa^2 n^{-4}\Phi_{\mathrm{D}})^{1/6} \ (\mathrm{nm})$$

where J is the overlap integral between the emission spectrum of the donor and the absorption spectrum of the acceptor, n is the refractive index of the solvent, Φ_{D} is the fluorescence quantum yield of the donor, and κ^2 is an orientational factor and is $\sim^2/_3$ for a randomly oriented donor. The calculated overlap integrals (J) for 4CP and URO between 500 and 700 nm are 4.66 $\times$ 10^{-15} and 5.05 $\times$ 10^{-15} cm^3/M, respectively (calculated according to ref 35). Using these values and Φ_{D} $\sim$0.04 (for both 4CP and URO),[37] $n = 1.332$ (for water), and $\kappa \sim 0.667$ (estimated from Zn cytochrome c–cytochrome c oxidase complex[36]), the rate constants are calculated to be 1.01 $\times$ 10^7 and 8.54 $\times$ 10^6 s^{-1} for energy transfer between 4CP and Cc and between URO and Cc, respectively. Since these rate constants are considerably smaller than the observed decay rate constants (7.87 $\times$ 10^8 and 2.63 $\times$ 10^8 s^{-1}, for 4CP and URO, respectively), we conclude that energy transfer does not make a significant contribution to the singlet-state quenching. Alternatively, both the singlet and triplet excited states of URO and 4CP exhibit favorable thermodynamics for ET to the heme group of the protein ($\Delta E = 1.1055$ and 1.135 V for singlet-state 4CP and URO, respectively, and $\Delta E = 1.06$ V for the triplet-state quenching of URO).[23,37] Thus, differences in the quenching rates reflect differences in the rate of photoinduced ET from the porphyrin to the heme.

The data further demonstrate that singlet-state quenching of URO is associated with distinct conformations/orientations, relative to triplet-state quenching. The fact that the URO–Cc complex does not display any rapid changes in absorbance at 550 nm suggests that the corresponding back ET rate is faster than the response time of our transient absorption instrument (i.e., $>1 \times 10^7$ s^{-1}). This is in contrast to the back ET rate measured for the triplet-state quenching, which is on the order of 10^6 s^{-1}. In the case of the 4CP–Cc complex, only singlet-state quenching is observed. Once again, no transient changes are observed at 550 nm, indicating that the back ET rate is either of the same order of magnitude or faster than the forward ET rate. One explanation for these results is that the porphyrins bind with different orientations/conformations with 4CP binding with an orientation favoring rapid forward and back ET

(resulting in singlet quenching) while URO binds with two distributions, one favoring rapid forward/backward ET (resulting in the singlet quenching) and one favoring slower forward/backward ET (resulting in triplet quenching).

The effects of orientation between donor and acceptor in nonadiabatic ET are described in the following expression for the rate constant:[13,14]

$$k_{\mathrm{et}} = (2\pi/h^2)|T_{\mathrm{AD}}|^2 \mathrm{FC}$$

where FC is the sum of thermally activated Franck–Condon factors for nuclear vibration and $|T_{\mathrm{AD}}|^2$ is the electronic coupling matrix element that contains orientation and distance factors. An expression for T_{AD} has been given previously as

$$T_{\mathrm{AD}} = (H_{\mathrm{AD}} - S_{\mathrm{DA}}H_{\mathrm{DD}})/(1 - |S_{\mathrm{DA}}|^2)$$

for a model in which the electron donor and acceptor are represented as isolated one-electron sites within oblate spheroidal potential wells. In this expression, $H_{\mathrm{AD}} = -V_{\mathrm{A}}<\Psi^{\mathrm{A}*}|\Psi^{\mathrm{D}}>$, $H_{\mathrm{DD}} = -V_{\mathrm{A}}<\Psi^{\mathrm{D}*}|\Psi^{\mathrm{D}}>$, and $S_{\mathrm{DA}} = <\Psi^{\mathrm{D}}|\Psi^{\mathrm{A}}>$. The wave functions, Ψ^{A} and Ψ^{D}, are written for an electron localized on the electron donor and acceptor, respectively and V_{A} is the potential function of the acceptor. A quantitative investigation using oblate spheroid potential functions (giving wave functions with nodal characteristics similar to that of porphyrin wave functions) revealed the orientational dependence of ET (Figure 10, top panel). Strong coupling (i.e., more facile ET) between donor and acceptor was noted for geometrys with $\Delta = \Lambda \sim 30$–$50°$.[13,14] In addition, when $\Delta = \Lambda \sim 70°$, it was predicted that the forward and back ET rates should be of comparable magnitude.

The model described above can also be applied to the porphyrin–Cc complexes discussed here by including an additional degree of freedom consisting of rotation of one ellipsoid about its axis while the other remains fixed (see Figure 10). In this case, the heme group of Cc represents one ellipsoid and the bound porphyrin represents the second ellipsoid. In addition, the distance between the two chromophores is approximately 12 Å, similar to the distance examined in the model system. The orientational differences in ET within the 4CP–
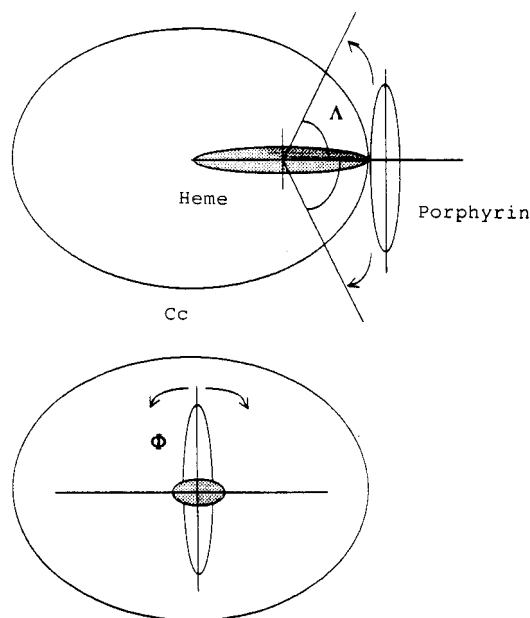
Conformational Modulation of Electron Transfer

J. Phys. Chem. B, Vol. 101, No. 40, 1997 **8019**

Figure 10. Model for electronic coupling between bound porphyrin and heme group of Cc. See text for details.

Cc and URO−Cc complexes can then be rationalized by qualitatively examining T_{BA} for each system. Since both porphyrins bind to the same region on Cc, we can conclude that Δ and Λ are likely to be the same for each system and since the ET reaction is quite facile for the 4CP−Cc, we suggest that $\Delta = \Lambda$ is in ∼30°, consistent with previous molecular modeling studies.[23] However, the rotational parameter Φ is distinct between the two complexes. In the case of the 4CP−Cc, the rapid ET rate is most likely due to a favorable overlap between the wave function on the heme and the wave function of the porphyrin. Rotation of the bound porphyrin on the surface of the protein results in poorer overlap and slower ET rates and is suggested for the URO−Cc complex. At this point, we cannot differentiate between an equilibrium distribution of URO orientations relative to the heme or whether the process is dynamic with the URO rotating on the surface of the protein through optimal electron transfer orientations.

Singlet-State Dynamics. Although the singlet state of the bound URO is only moderately quenched, those chromophores that are quenched exhibit a distribution of quenched lifetimes. On the other hand, the singlet state of 4CP displays only a single quenched lifetime within the complex. There are several possible explanations for the presence of the URO lifetime distribution. One possibility is that the URO is bound statically with several orientations centered around the optimal orientation. If this were the case, it would be difficult to rationalize why the 4CP would not also bind with a similar range of distributions since both porphyrins bind to the same region on the protein.

An alternative scenario is that the distribution of lifetimes associated with the bound URO arises from dynamic motions of the bound URO due to the flexibility of the URO peripheral side chains. It has been suggested by Wicks[38] that Ni^{II}URO bound to the surface of cationic cetyltrimethylammonium bromide (CTAB) micelles does so with a conformation in which the acidic side chains bend out of plain toward the surface of the micelle. Thus, the porphyrin plane comprising the conjugated ring system is farther away from the surface than would be anticipated with more rigid side groups (Figure 11). In addition, this orientation is likely to be flexible with the porphyrin plane dynamically moving toward and away from the micelle surface. Applying this model to the protein-bound
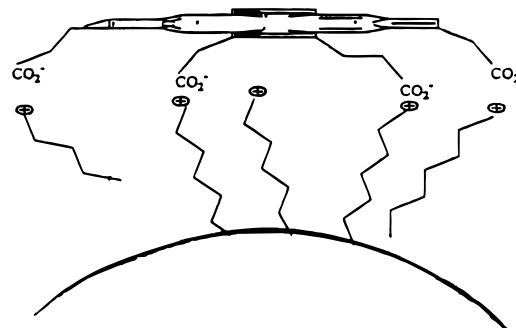

Figure 11. Model describing conformational interactions between the side chains of URO and the surface of Cc (adapted from ref 38).

URO leads to a conformation in which the flexible porphyrin side chains associate electrostatically with protein peripheral lysine groups analogous to the Ni^{II}URO/CTAB system and would be expected to exhibit similar dynamics. In contrast, the 4CP has very rigid side groups giving rise to a much more rigid complex.

Implications for Protein−Protein Intermolecular ET. Both distance and orientation play a key role in modulating intermolecular ET in proteins. It is now becoming evident that the surface charge distribution associated with each protein is largely responsible for directing complex formation. Thus, such electrostatic interactions (expressed through mutual protein dipole orientations) guide each protein within the complex to the proper distance and orientation required for facile ET. As discussed previously, these complexes are very dynamic and factors such as surface diffusion can also modulate the ET rate once the complex has formed. The complexes formed between 4CP−URO and Cc share common features with protein−protein complexation. Specifically, both involve significant electrostatic interactions between carboxylic acid residues on one protein/porphyrin and lysine residues on Cc. It is of specific interest to note that the rigid carboxylic acid groups associated with the 4CP severely restrict surface dynamics while the more flexible groups associated with URO (and similar to carboxylic amino acids) facilitate surface motions which modulate the rate of ET between the donor and acceptor. It is tempting to speculate that this flexibility may be of specific importance in the complex regulation of interprotein ET via docking interactions.

In summary, the data presented here directly demonstrate the role of surface orientation between ET donor and acceptor in modulating intermolecular ET in biological molecules. In addition, the flexibility of the groups involved in complex formation is also demonstrated to have an affect on the electron transfer rate. The conformational flexibility is likely a dynamic affect while the orientational modulation may be either static or dynamic.

References and Notes

(1) Barbara, P. F.; Meyer, T. J.; Ratner, M. A. *J. Phys. Chem.* **1996**, *100*, 13148−13168.

(2) Marcus, M. A.; Sutin, N. *Biophys. Biochim. Acta* **1985**, *811*, 265−322.

(3) Boxer, S. G. *Annu. Rev. Biophys. Biophys. Chem.* **1990**, *19*, 267–299.

(4) Larsson, S. *J. Chem. Soc., Faraday Trans. 2* **1983**, *79*, 1375–1388.

(5) McLendon, G.; Hake, R. *Chem. Rev.* **1992**, *92*, 481–490.

(6) Siddarth, P.; Marcus, R. A. *J. Phys. Chem.* **1990**, *94*, 8430–8434.

(7) Wuttke, D. S.; Bjerrum, M. J.; Chang, I.-J.; Winkler, J. R.; Gray, H. B. *Biochim. Biophys. Acta* **1992**, *1101*, 168–170.

(8) Isied, S. S.; Vassilian, A.; Wishart, J. F. *J. Am. Chem. Soc.* **1988**, *110*, 635–637.

(9) Gaines, G. L.; O'Neal, M. P.; Svec, W. A.; Niemczyk, M. P.; Wasielewski, M. R. *J. Am. Chem. Soc.* **1991**, *113*, 719–721.

(10) Mikkelsen, K. V.; Ulstrup, J.; Zakaraya, M. G. *J. Am. Chem. Soc.* **1989**, *111*, 1315–1319.

(11) Osuka, A.; Maruyama, K.; Mataga, N.; Asahi, T.; Yamazaki, I.; Tamai, N. *J. Am. Chem. Soc.* **1990**, *112*, 4958–4959.

(12) Rips, I.; Jortner, J. *J. Chem. Phys.* **1987**, *87*, 2090–2104.

(13) Cave, R. J.; Siders, P.; Marcus, R. A. *J. Phys. Chem.* **1986**, *90*, 1436–1444.

(14) Siders, P.; Cave, R. J.; Marcus, R. A. *J. Chem. Phys.* **1984**, *81*, 5613–5624.

(15) McLendon, G. *Struct. Bonding* **1991**, *75*, 160–174.

(16) Nuevo, M. R.; Chu, H.–H.; Vitello, L. B.; Erman, J. E. *J. Am. Chem. Soc.* **1993**, *115*, 5873–5874.

(17) Mauk, M. R.; Ferrer, J. C.; Mauk, A. G. *Biochemistry* **1994**, *33*, 12609–12614.

(18) Corin, A. F.; McLendon, G.; Zhang, Q.; Hake, R. A.; Falvo, J.; Lu, K. S.; Ciccarelli, R. B.; Holzschu, D. *Biochemistry* **1991**, *30*, 11585–11595.

(19) Wallin, S. A.; Stemp, E. D. A.; Everest, A. M.; Nocek, J. M.; Netzel, T. L.; Hoffman, B. M. *J. Am. Chem. Soc.* **1991**, *113*, 1842–1844.

(20) Zhou, J. S.; Kostic, N. M. *J. Am. Chem. Soc.* **1992**, *114*, 3562–3563.

(21) Zhou, J. S.; Kostic, N. M. *Biochemistry* **1993**, *32*, 4539–4546.

(22) Clark-Ferris, K. K.; Fisher, J. *J. Am. Chem. Soc.* **1985**, *107*, 5007–5008.

(23) Zhou, J. S.; Granada, E. S. V.; Leontis, N. B.; Rodgers, M. A. J. *J. Am. Chem. Soc.* **1990**, *112*, 5074–5080.

(24) Zhou, J. S.; Rodgers, M. A. J. *J. Am. Chem. Soc.* **1991**, *113*, 7728–7734.

(25) Margoliash, E.; Frohwirt, N. *Biochem. J.* **1959**, *71*, 570–572.

(26) Fuhrhop, J.-H.; Smith, K. M. *Laboratory Methods in Porphyrin and Metalloporphyrin Research*, Elsevier Publishing: **1975**.

(27) Larsen, R. W.; Jasuja, R.; Hetzler, R. K.; Muraoka, P. T.; Andrada, V. G.; Jameson, D. M. *Biophys. J.* **1996**, *70*, 443–452.

(28) Vaugn, W. M.; Weber, G. *Biochemistry* **1970**, *9* (3), 464–473.

(29) Cho, K. C.; Che, C. M.; Ng, K. M.; Choy, C. L. *J. Am. Chem. Soc.* **1986**, *108*, 2814–2818.

(30) Waldmeyer, B.; Bosshard, H. R. *J. Biol. Chem.* **1985**, *260*, 5184–5190.

(31) Koppeno, W. H.; Margoliash, E. *J. Biol. Chem.* **1982**, *257*, 4426–4437.

(32) Charney, E. *The Molecular Basis for Optical Activity*; Wiley and Sons: New York, 1979.

(33) Hsu, M.-C.; Woody, R. W. *J. Am. Chem. Soc.* **1971**, *93*, 5–3525.

(34) Blauer, G.; Sreerama, N.; Woody, R. W. *Biochemistry* **1993**, *32*, 6674–6679.

(35) Campbell, I. D.; Dwek, R. A. *Biological Spectroscopy*; Benjamin/Cummings: Menlo Park, CA, 1984.

(36) Dockter, M. E.; Steinemann, A.; Schatz, G. *J. Biol. Chem.* **1978**, *253*, 311–317.

(37) Kalyanasundaram, K.; Neumann-Spallart, M. *J. Phys. Chem.* **1982**, *86*, 7728–7734.

(38) Wicks, B. S. Dissertation, University of Toledo, Toledo, OH, 1994.